ROBOT TRAJECTORY PLANNING

DARINA HRONCOVA[1], PETER JAN SINCAK[1], TOMAS MERVA[1], ROMAN MYKHAILYSHYN[2]

[1]Technical University of Kosice, Faculty of Mechanical Engineering, Kosice, Slovakia

[2]Texas Robotics, College of Natural Sciences and the Cockrell School of Engineering, The University of Texas at Austin, Austin, TX 78712, USA

DOI: 10.17973/MMSJ.2022_11_2022093

darina.hroncova@tuke.sk

The paper deals with the kinematic analysis of the robot model. The matrix method of kinematic analysis is used. The robot mechanism is an open kinematic chain. The position, velocity and acceleration vector of the end point of the robot arm is determined in the Matlab program. Computer simulation is also performed in the MSC Adams program.

KEYWORDS

trajectory, end – effector, robot, computer simulation, kinematics, symbolic form, matrix method, MSC Adams/View, Matlab/Simulink

1 INTRODUCTION

The task of the kinematic solution of coupled mechanical systems is to investigate the dependence of the coordinates of the driven kinematic pairs on the coordinates of the global coordinate system. The effort is to determine the movement of its important points and members, to determine the position, corresponding velocities and accelerations.

We can solve kinematic analysis of mechanisms in analytical, graphical and experimental ways. The development of computers broadens the application of analytical methods. The connection of computers with the means of displaying calculation results on the screen or on paper largely eliminates the shortcomings of analytical methods resulting from the low visibility of the obtained results. Computers with their software enable the most accurate determination of the parameters [Smrcek 2003, Karban 2006, Vagas 2011, Abramov 2015, Bozek 2014, Nikitin 2022, Virgala 2014, Garcia 2015, Semjon 2016 and 2020, Sapietova 2018, Saga 2020, Segota 2020, Kuric 2021].

2 DESIGNED CONCEPTS OF ROBOT KINEMATICS

Analytical methods of solving mechanisms are based on the use of methods of analytical geometry, tensor and matrix calculus, complex variable and other areas of mathematics. These methods are connected to coordinate systems and lead to scalar equations for the quantities being sought.

However, matrix methods are often the most advantageous for constructing algorithms of a general nature for solving kinematic and force quantities of mechanisms of different composition. Matrix notation is compact, illustrative, and suitable for use in a computer environment. It enables an easy transition from symbolic equations to scalar equations and is suitable for numerical methods applicable on a computer. The theory of simple open kinematic chains has a direct application in the kinematic analysis of various manipulators and robots, which are often formed by the mentioned chains. We can decompose the motion of two bodies into a finite number of basic motions [Brat 1981, Stejskal 1996, Virgala 2012, Hroncova 2012 and 2014, Delyova 2014, Mikova 2014, Serrano 2015, Xiong 2018].

The kinematic diagram of one of such manipulators is shown in Fig. 1. The following parts of the post are devoted to its solution.

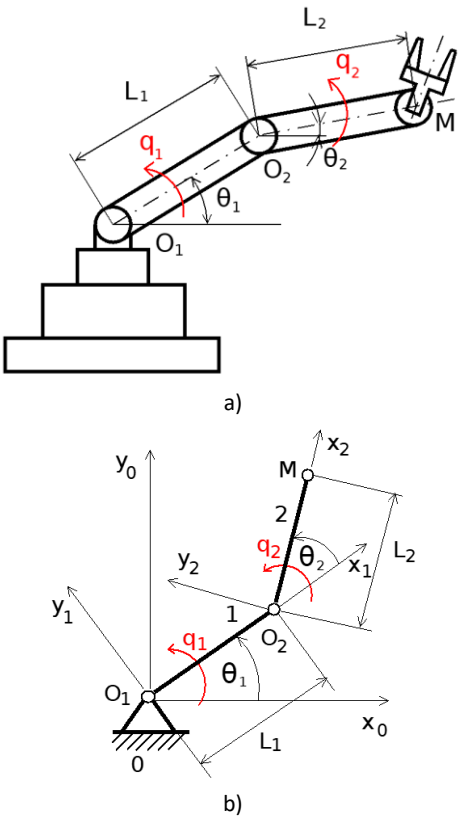

Figure 1. a) Manipulator with a two-link robotic arm with generalized coordinates $q_1 = \Theta_1$, $q_2 = \Theta_2$, b) kinematic scheme of two-link robotic arm with generalized coordinates

3 EVALUATION OF BIPEDAL ROBOT CONCEPTS

The solution to the movement of the manipulation arm in the shape shown in Fig. 1, composed of two members, can be presented as follows: Member 1 of length L_1 rotates around axis z_1 by angle θ_1 and member 2 of length L_2 rotates around axis z_2 by angle θ_2 (Fig. 1). It is necessary to investigate the absolute movement of the end point M and to determine the position vector $\mathbf{r_{0M}}$ of the point M with respect to the base 0 and to express the velocity $\mathbf{v_{0M}}$ and the acceleration $\mathbf{a_{0M}}$ of the point M with respect to the base 0. We determine the position of point M using the transformation matrices of basic movements.

When solving the position of the end point of the manipulator, we encounter the solution of the inverse problem of kinematics. Considering the required location of the end point M (Fig. 2) of the robotic arm, we need to determine what the angles of rotation of the joints should be so that the end point M is placed at the desired location. We calculate the inverse kinematics problem. When solving the motion of two members, there is usually more than one solution as shown in Fig. 2.

This is a typical problem in robotics that must be solved to control the movement of a robotic arm to perform the tasks we require. In a two-dimensional space with two terms L_1 and L_2 bound by rotational bonds and given the required endpoint coordinate M, the problem reduces to finding both angles. The first angle θ_1 is between the first arm and the base. The second angle θ_2 is between the first arm and the second arm. For the solution, we will use equations in the form:

$$x_L = L_1 \cos\theta_1 + L_2 \cos(\theta_1 + \theta_2) \quad (1)$$

$$y_L = L_1 \sin\theta_1 + L_2 \sin(\theta_1 + \theta_2) \quad (2)$$

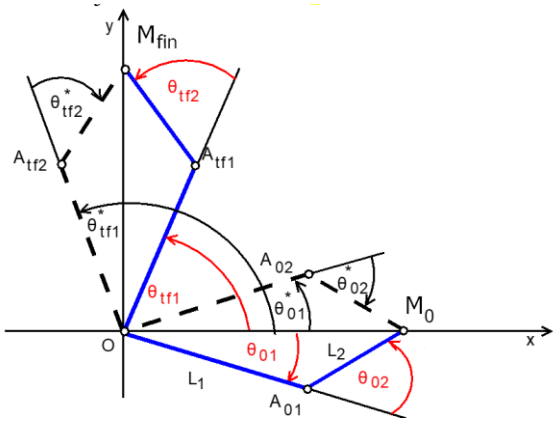

Figure 2. The starting M_0 and ending M_{fin} position of the point M

We determine the angles of both arms at the beginning θ_{01}, θ_{02} at time t = 0 and at the end of the movement θ_{tf1}, θ_{tf2} at time t = t_{fin} (the final time will be denoted also with t_{fin} or t_{tf}) in Fig. 3. From equations (1) and (2) with the known position of the starting point M_0 at time t = 0 and at the end position of point Mfin, at time t=tfin we calculate individual angles θ_{01}, θ_{02} at the starting position x_{M0} and y_{M0} of point M_0. We proceed in the same way for the final position x_{Mtf} and y_{Mtf} of the point M_{fin}, where we obtain the angles of both arms θ_{tf1}, θ_{tf2}.
When solving a direct problem of kinematics, we determine the position of the end point M, which is described by equations (1) to (2) and obtain the trajectory of the point M.

4 FORWARD KINEMATICS OF THE RR MANIPULATOR

The two-member robotic arm is formed by members 1 and 2 according to Fig. 1 with lengths L_1 and L_2. The arms are connected by one rotary kinematic pair to the frame and are connected to each other by a second rotary kinematic pair. The drives are stored in rotary kinematic pairs. The rotation angle in kinematic pairs is indicated by the angles θ_1 and θ_2.
We are looking for the time course of angular rotations θ_1 and θ_2 in the form of a 5th degree polynomial:

$$\theta_1(t) = a_1 t^5 + a_2 t^4 + a_3 t^3 + a_4 t^2 + a_5 t + a_6 \quad (3)$$

$$\theta_2(t) = b_1 t^5 + b_2 t^4 + b_3 t^3 + b_4 t^2 + b_5 t + b_6 \quad (4)$$

where $a_6 = \theta_1(t = 0)$ a b6 = $\theta_2(t = 0)$ are the initial angles of rotation at time t = 0:

$$\theta_1(t) = a_1 t^5 + a_2 t^4 + a_3 t^3 + a_4 t^2 + a_5 t + \theta_1(0) \quad (5)$$

$$\theta_2(t) = b_1 t^5 + b_2 t^4 + b_3 t^3 + b_4 t^2 + b_5 t + \theta_2(0) \quad (6)$$

from which we will determine the vector coefficients to ensure the desired movement:

$$\mathbf{a} = [a_1 \ a_2 \ a_3 \ a_4 \ a_5]^T \quad (7)$$

$$\mathbf{b} = [b_1 \ b_2 \ b_3 \ b_4 \ b_5]^T \quad (8)$$

For the required initial coordinates (x, y) at time t = 0 and the required final coordinates at time $t = t_{fin} = tf$ the required value for the angles $\theta_1(t = 0)$, $\theta_2(t = 0)$, $\theta_1(t = tf)$, $\theta_2(t = tf)$ can be found using trigonometry. For the given values of the angles $\theta_1(0)$, $\theta_1(tf)$, a set of equations will be compiled in matrix form and solved for the coefficients a. Similarly, for the given values of the angles $\theta_2(0)$, $\theta_2(tf)$, a set of equations will be compiled in matrix form and solved for coefficients b. These results will be printed and used to plot the trajectory of the end point M. Side constraints on the motion of the robot arm are that the velocity and acceleration of the members are zero at the known initial and desired final positions. This indicates that the angular velocity and angular acceleration of the two angles are zero at time t = 0 and $t = tf$.
The coefficients in these polynomials (3) and (4) are determined from the initial and final conditions for the movement of the end point M, where a_4 = 0, a_5 = 0, b_4 = 0, b_5 = 0. Their degree is chosen in such a way that with them they expressed all the prescribed conditions. After setting the initial and final conditions and solving the system of equations, the other coefficient values are as follows: a_1 = 0.3272, a_2 = -1.6362, a_3 = 2.1817, b_1 = -0.0982, b_2 = 0.4909, b_3 = -0.6545. After determining them, we can represent the trajectory of the end point M. With the known values of the angles, we determine the position of the point. We solve the direct task of kinematics. When the manipulator moves with arms of length L_1 = 0.4 meters and L_2 = 0.3 meters and at the position of points θ_{10} = -38°, θ_{20} = 98°, θ_{1fin} = 62°, θ_{2fin} = 68°, the position of point M during the movement is shown in Fig. 3.

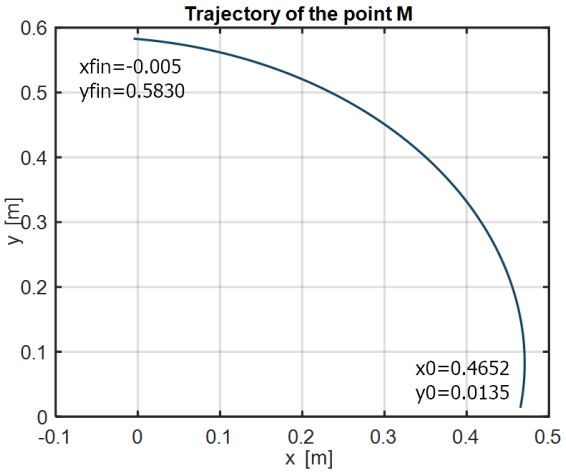

Figure 3. Trajectory of the point M

Representation of endpoint position for parameters:

```
L1 = 0.4;
L2 = 0.3;
theta1 = 0:0.1:(3*pi)/2;
theta2 = 0:0.1:(3*pi)/2;
```

for all combinations of positions of angles θ_1 from 0 to (3/2)π and angle θ_2 from 0 to (3/2)π in Fig. 4:

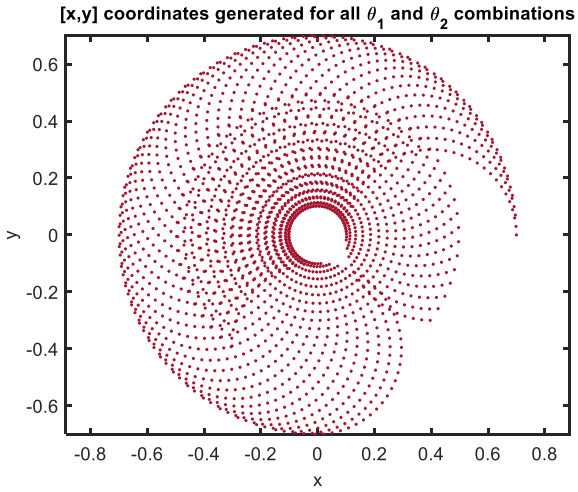

Figure 4. Coordinates x-y for all θ_1 and θ_2

The course of the angular quantities with the known trajectory of the end point M in Fig. 3 of the end point M is shown in Fig. 5.

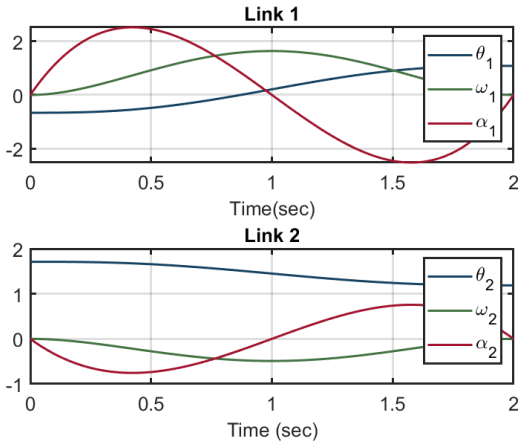

Figure 5. Course of angular quantities of angles θ_1 and θ_2, angular velocities ω_1 and ω_2 and angular accelerations α_1 and α_2

The block diagram for solving the problem of inverse dynamics in SimMechanics for calculating moments in individual joints is in Fig. 6.

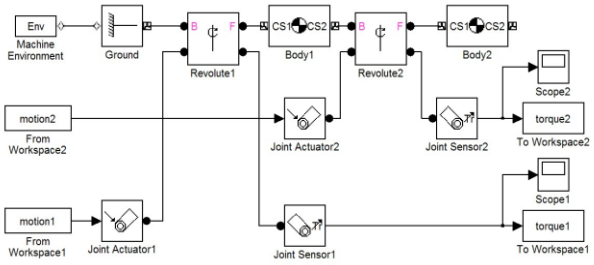

Figure 6. Scheme in SimMechanics to determine the moments τ_1 and τ_2 as a function of time in the joint of member 1 and 2

By solving the inverse problem of dynamics using SimMechanics in the Matlab/Simulink program, we can determine the course of moments τ_1 and τ_2 (Fig. 7) in the individual joints of the two-member arm of the manipulator from Fig. 1.

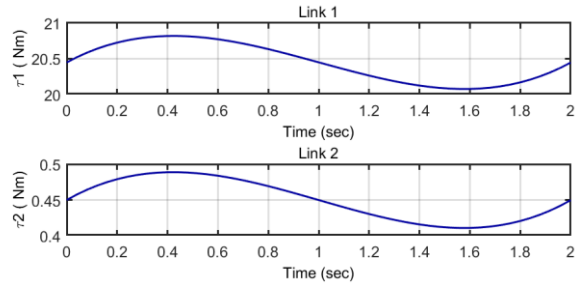

Figure 7. Courses of moments τ_1 and τ_2 depending on time in the joint of member 1 and member 2

The maximum magnitude of moments in the joints of the robotic arm of lengths L_1 and L_2 is τ_1 = 20.8183 Nm and τ_2 = 0.4888 Nm.

5 TRAJECTORY OF THE END POINT, COURSE OF ANGULAR QUANTITIES AND MOMENTS IN KINEMATIC PAIRS

We are looking for the course of the trajectory of the manipulation arm with member lengths L_1=0.4m, L_2=0.3m (Fig. 1) determined during its movement from the starting point A to points B, C and D and back to point A. The position of points A to D is given in Tab.1

Table 1. Coordinates of the points A, B, C, D

	A	B	C	D
x_i [m]	0.4	0.7	0.4	0.1
y_i [m]	-0.3	0.0	0.3	0.0

When moving from point A to point B, from point B to point C and finally from point D to point A, we expect that the end point will draw a closed curve, which will be a circle (Fig. 8). Arm rotation angles in the initial and final positions are calculated using the solution of the inverse kinematics problem and their size is in Tab.2.

Table 2. Sizes of initial and final rotation angles when moving along trajectories between points A-B, B-C, C-D, D-A

	A-B	B-C	C-D	D-A
Θ_{10}	-74°	0°	0°	0°
Θ_{20}	90°	0°	90°	-90°
Θ_{1tf}	0°	74°	0°	0°
Θ_{2tf}	0°	-90°	180°	-180°

The shape of the trajectory in the movement from point A to point B, from point B to point C and finally from point D to point A is, as expected, the circle in Fig. 8.

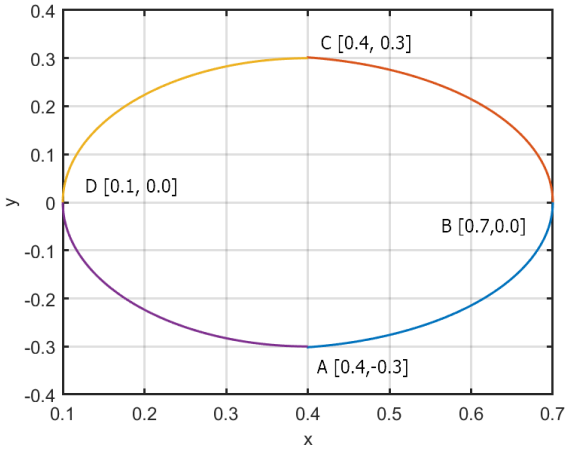

Figure 8. Trajectory of point M (from–to): A-B, B-C, C-D, D-A

From the known position of the end point of the members at the beginning of the movement and at the end of the movement, by interpolating the 5th degree polynomial, the rotation angles, angular velocity and angular acceleration of both arms are determined, the magnitude of which is shown graphically in Fig. 9.

When solving the inverse problem of dynamics, we then determine the magnitudes of moments (Fig. 10) in individual kinematic pairs of both arms. Based on the results obtained by computer simulation, we can build a real model and design servo drives based on calculations. When designing servo drives, it is necessary to take into account the maximum magnitude of the load on the mechanical system when handling various loads [Trojanova 2021]. It is necessary to oversize the drives for specific requirements intended for the specific purpose of using the manipulator.

From the magnitude of the moments in Tab. 3, it is clear that when moving from point C to point D and then from D to the starting point A, larger moments are needed in both kinematic pairs than when moving from point A to B and then from B to point C.

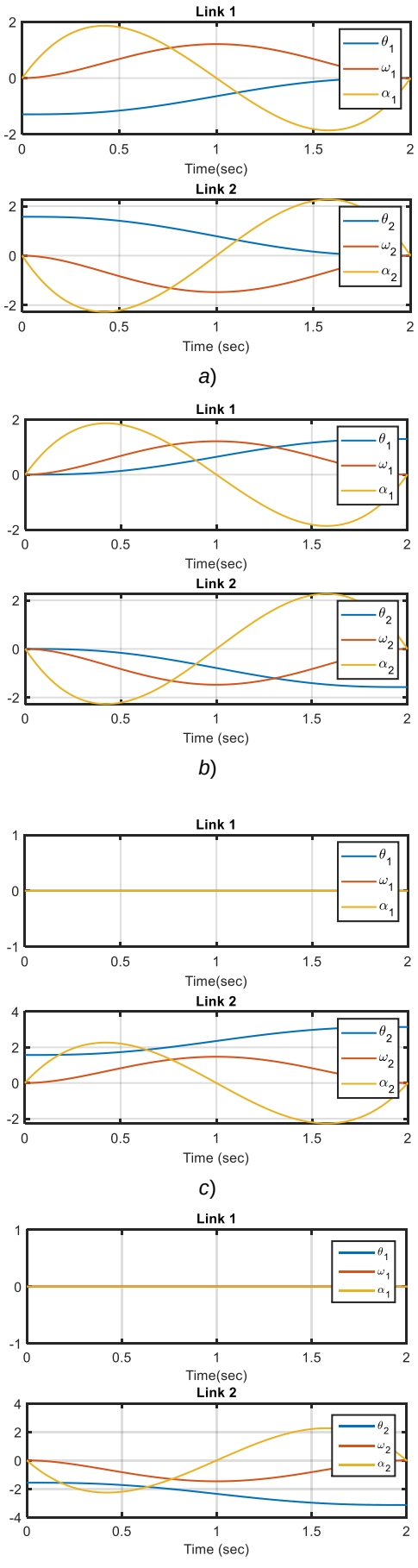

Figure 9. Course of angular quantities of angles θ_1 and θ_2, angular velocities ω_1 and ω_2 and angular accelerations α_1 and α_2 for the section: a) A-B, b) B-C, c) C-D, d) D-A

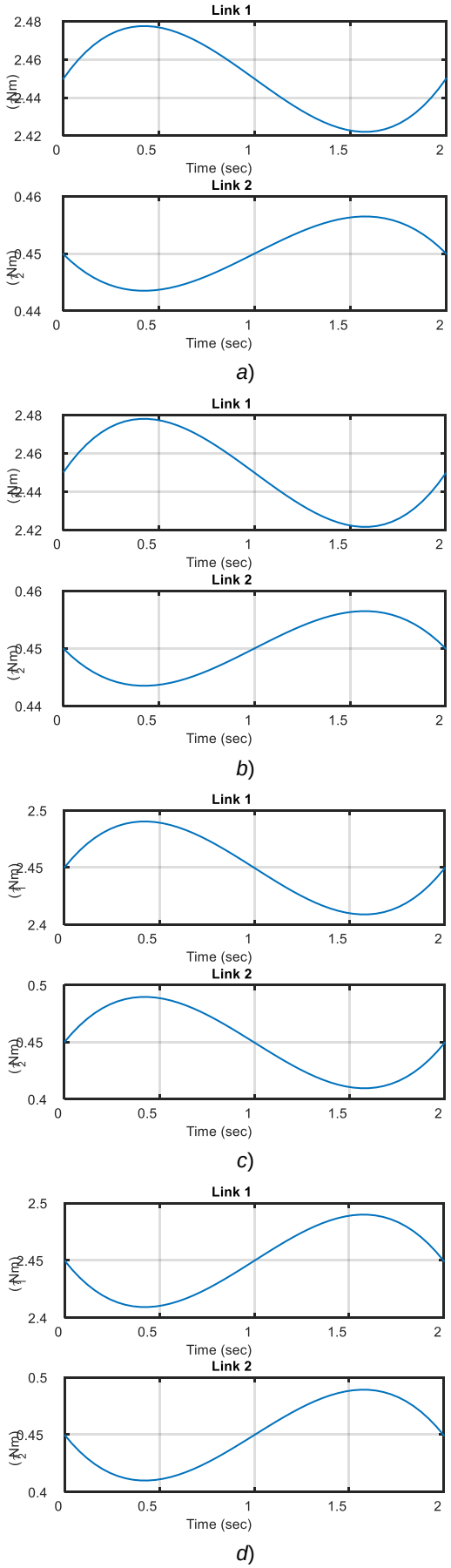

Figure 10. Courses of moments τ_1 and τ_2 depending on time in the joint of member 1 and member 2 for the section: a) A-B, b) B-C, c) C-D, d) D-A

Table 3. The maximum size of the moments τ_{1max} and τ_{2max} in the section between the points A-B, B-C, C-D, D-A

	A-B	B-C	C-D	D-A
τ_{1max} [Nm]	2.4775	2.478	2.4903	2.4899
τ_{2max} [Nm]	0.4565	0.4565	0.4896	0.4892

6 MODEL OF THE RRRR MANIPULATOR

Mechanical systems of manipulators mostly represent open kinematic chains. The manipulator in Fig. 11 is composed of a base 0 on which the stand 1 is fixed and a manipulation arm, composed of two members 2 and 3, at the end of which the effector 4 is connected.

We introduce coordinate systems in individual members according to Fig. 11. The movement of member 1 with respect to the base 0 is rotated by an angle θ_{01}. The coordinate system O_1, x_1, y_1, z_1 of member 1 is rotated by an angle θ_{01} with respect to the base coordinate system O_0, x_0, y_0, z_0. We choose the generalized coordinate $q_1 = \theta_{01}$.

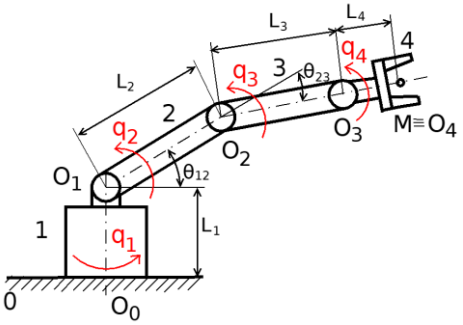

Figure 11. Model of RRRR manipulator on a fixed stand with generalized coordinates $q_1 = \Theta_{01}$, $q_2 = \Theta_{12}$, $q_3 = \Theta_{23}$, $q_4 = \Theta_{34}$

The coordinate system O_2, x_2, y_2, z_2 of member 2 is rotated by the angle θ_{12}. The coordinate system O_2, x_2, y_2, z_2 of member 2 with respect to the coordinate system O_1, x_1, y_1, z_1 is rotated by the angle θ_{12} and we choose the generalized coordinate $q_2 = \theta_{12}$. The coordinate system O_3, x_3, y_3, z_3 of the member 3 with respect to the coordinate system O_2, x_2, y_2, z_2 rotated by the angle θ_{23} and we choose the generalized coordinate $q_3 = \theta_{23}$. The coordinate system O_4, x_4, y_4, z_4 of member 4 is rotated by the angle θ_{34} with respect to the coordinate system O_3, x_3, y_3, z_3. We choose the generalized coordinate $q_4 = \theta_{34}$. The position of the endpoint M in the space of member 4 is $r_{4M} = [0\ 0\ 0\ 1]^T$. Our task is to investigate the absolute movement of the point M with respect to the basis 0.

7 MATRIX METHOD FOR SOLVING THE KINEMATICS OF A ROBOT MODEL

There are several methods for expressing the geometric arrangement of arms and joints of manipulators. They try to define coordinate systems representing the individual arms of the manipulator and their mutual positional transformation in a simple and systematic way. The positional transformation of two consecutive coordinate systems depends on the given constant geometric parameters, which include the geometric shape of the arms, the joints and their mutual configuration, and on the joint coordinates, which include the current position of the joints. Among the most famous methods is the Denavit-Hartenberg method. Using the Denavit–Hartenberg parameters (D-H parameters) (Fig. 12), a table of parameters (Tab. 4) is compiled on the basis of which the position of the end point of the manipulator arm is determined using the matrix method.

Using the Hartenberg-Denavit method, mutual position is expressed using four parameters of two lengths a_i, d_i and two angles α_i, Θ_i, which is shown in Fig. 12.

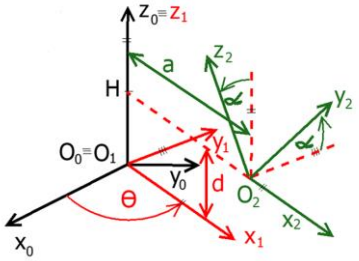

Figure 12. Denavit - Hartenberg parameters

The resulting matrix of the transformation of the coordinate system O_i to O_{i+1} is in the form:

$$\boldsymbol{T}_{i,i+1} = \boldsymbol{T}_{Z3}(d_i) \cdot \boldsymbol{T}_{Z6}(\theta_i) \cdot \boldsymbol{T}_{Z1}(a_i) \cdot \boldsymbol{T}_{Z4}(\alpha_i) \tag{9}$$

where:

$\boldsymbol{T}_{Z3}(d_i)$ - expresses the translational movement in the direction of the axis z with d_i,

$\boldsymbol{T}_{Z6}(\Theta_i)$ – rotational movement around an axis z with angle Θ_i,

$\boldsymbol{T}_{Z1}(a_i)$ – translational movement in the direction of the axis x with a_i,

$\boldsymbol{T}_{Z4}(\alpha_i)$ – rotational movement around the axis x with angle α_i.

The form of the matrix results from the type of joint:

$$\boldsymbol{T}_{Z3}(d_i) = \begin{bmatrix} 1 & 0 & 0 & 0 \\ 0 & 1 & 0 & 0 \\ 0 & 0 & 1 & d_i \\ 0 & 0 & 0 & 1 \end{bmatrix} \tag{10}$$

$$\boldsymbol{T}_{Z6}(\theta_i) = \begin{bmatrix} \cos\theta_i & -\sin\theta_i & 0 & 0 \\ \sin\theta_i & \cos\theta_i & 0 & 0 \\ 0 & 0 & 1 & 0 \\ 0 & 0 & 0 & 1 \end{bmatrix} \tag{11}$$

$$\boldsymbol{T}_{Z1}(a_i) = \begin{bmatrix} 1 & 0 & 0 & a_i \\ 0 & 1 & 0 & 0 \\ 0 & 0 & 1 & 0 \\ 0 & 0 & 0 & 1 \end{bmatrix} \tag{12}$$

$$\boldsymbol{T}_{Z4}(\alpha_i) = \begin{bmatrix} 1 & 0 & 0 & 0 \\ 0 & \cos\alpha_i & -\sin\alpha_i & 0 \\ 0 & \sin\alpha_i & \cos\alpha_i & 0 \\ 0 & 0 & 0 & 1 \end{bmatrix} \tag{13}$$

After substitution, the resulting transfer matrix is:

$$\boldsymbol{T}_{i-1,i} = \boldsymbol{T}_{Z3}(d_i) \cdot \boldsymbol{T}_{Z6}(\theta_i) \cdot \boldsymbol{T}_{Z1}(a_i) \cdot \boldsymbol{T}_{Z4}(\alpha_i) = \begin{bmatrix} \cos\theta_i & -\cos\alpha_i\sin\theta_i & \sin\alpha_i\sin\theta_i & a_i\cos\theta_i \\ \sin\theta_i & \cos\alpha_i\cos\theta_i & -\sin\alpha_i\cos\theta_i & a_i\sin\theta_i \\ 0 & \sin\alpha_i & \cos\alpha_i & d_i \\ 0 & 0 & 0 & 1 \end{bmatrix} \tag{14}$$

For the robot model in Fig. 13 is the form of the Denavit–Hartenberg parameters shown in Tab.4.

Table 3. Denavit-Hartenberg parameters for the manipulator RRRR

i	α_i [°]	a_i [m]	Θ_i [°]	d_i [m]
0	π/2	0	q_1	L_1
1	0	L_2	q_2	0
2	0	L_3	q_3	0
3	0	L_4	q_4	0

We are looking for the position, velocity and acceleration of point *M*. Then the drifting motion of this member is determined by the motion of point *M* and expressed using the basic decomposition to the reference point *M* and described by the equation:

$$r_{0M} = \prod_{i=0}^{3} T_{i,i+1} \cdot r_{4M} \quad (15)$$

The relative spherical motion is described by the transformation matrix:

$$T_{04} = \prod_{i=0}^{3} T_{i,i+1} \quad (16)$$

We will write the transformation matrices between the individual coordinate systems in kinematic pairs using the transformation matrices of basic movements. The matrix equation of the trajectory of point M with respect to the coordinate system of the base 0:

$$r_{0M} = T_{04} \; r_{4M} \quad (17)$$

where matrix $\mathbf{T_{04}}$:

$$T_{04} = T_{01} \; T_{12} \; T_{23} \; T_{34} \quad (18)$$

$$r_{0M} = T_{01} \; T_{12} \; T_{23} \; T_{34} \; r_{4M} \quad (19)$$

$$r_{4M} = [0\;0\;0\;1]^T \quad (20)$$

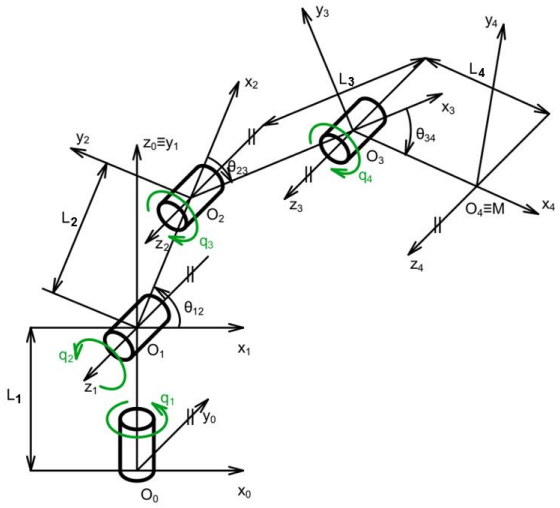

Figure 13. Kinematic scheme of the manipulator RRRR

The transformation between the coordinate system of base member 0 and member 1 is described by a matrix T01, where $q_1 = \Theta_{01}$:

$$T_{01} = T_{Z3}(L_1)\; T_{Z6}(q_1)\; T_{Z4}(\pi/2) \quad (21)$$

The form of the matrices results from the type of joint:

$$T_{Z3}(L_1) = \begin{bmatrix} 1 & 0 & 0 & 0 \\ 0 & 1 & 0 & 0 \\ 0 & 0 & 1 & L_1 \\ 0 & 0 & 0 & 1 \end{bmatrix} \quad (22)$$

The form of the matrices, when we mark *s*=sin, *c*=cos:

$$T_{Z6}(q_1) = \begin{bmatrix} c\,q_1 & -s\,q_1 & 0 & 0 \\ s\,q_1 & c\,q_1 & 0 & 0 \\ 0 & 0 & 1 & 0 \\ 0 & 0 & 0 & 1 \end{bmatrix} \quad (23)$$

after installation $q_1 = \pi/2$:

$$T_{Z4}(\pi/2) = \begin{bmatrix} 1 & 0 & 0 & 0 \\ 0 & c(\pi/2) & -s(\pi/2) & 0 \\ 0 & s(\pi/2) & c(\pi/2) & 0 \\ 0 & 0 & 0 & 1 \end{bmatrix} \quad (24)$$

after calculation:

$$T_{Z4}(\pi/2) = \begin{bmatrix} 1 & 0 & 0 & 0 \\ 0 & 0 & -1 & 0 \\ 0 & 1 & 0 & 0 \\ 0 & 0 & 0 & 1 \end{bmatrix} \quad (25)$$

The transformation between the coordinate system of member 1 and member 2 is described by the matrix T_{12}, when $q_2 = \Theta_{12}$:

$$T_{12} = T_{Z6}(q_2) T_{Z1}(L_2) \quad (26)$$

The form of the matrices results from the type of joint:

$$T_{Z6}(q_2) = \begin{bmatrix} c\,q_2 & -s\,q_2 & 0 & 0 \\ s\,q_2 & c\,q_2 & 0 & 0 \\ 0 & 0 & 1 & 0 \\ 0 & 0 & 0 & 1 \end{bmatrix} \quad (27)$$

$$T_{Z1}(L_2) = \begin{bmatrix} 1 & 0 & 0 & L_2 \\ 0 & 1 & 0 & 0 \\ 0 & 0 & 1 & 0 \\ 0 & 0 & 0 & 1 \end{bmatrix} \quad (28)$$

The transformation between the coordinate system of member 2 and member 3 is described by a matrix T_{23}, when $q_3 = \Theta_{23}$:

$$T_{23} = T_{Z6}(q_3) T_{Z1}(L_3) \quad (29)$$

The form of matrix:

$$T_{Z6}(q_3) = \begin{bmatrix} c\,q_3 & -s\,q_3 & 0 & 0 \\ s\,q_3 & c\,q_3 & 0 & 0 \\ 0 & 0 & 1 & 0 \\ 0 & 0 & 0 & 1 \end{bmatrix} \quad (30)$$

$$T_{Z1}(L_3) = \begin{bmatrix} 1 & 0 & 0 & L_3 \\ 0 & 1 & 0 & 0 \\ 0 & 0 & 1 & 0 \\ 0 & 0 & 0 & 1 \end{bmatrix} \quad (31)$$

The transformation between the coordinate system of member 3 and member 4 is described by a matrix T_{34}, when $q_4 = \Theta_{34}$:

$$T_{34} = T_{Z6}(q_4)\; T_{Z1}(L_4) \quad (32)$$

The form of matrix:

$$T_{Z6}(q_4) = \begin{bmatrix} c\,q_4 & -s\,q_4 & 0 & 0 \\ s\,q_4 & c\,q_4 & 0 & 0 \\ 0 & 0 & 1 & 0 \\ 0 & 0 & 0 & 1 \end{bmatrix} \quad (33)$$

$$T_{Z1}(L_4) = \begin{bmatrix} 1 & 0 & 0 & L_4 \\ 0 & 1 & 0 & 0 \\ 0 & 0 & 1 & 0 \\ 0 & 0 & 0 & 1 \end{bmatrix} \quad (34)$$

The position vector r_{0M} of the point M of member 4 in the coordinate system of the base 0 using the basic matrices:

$$r_{0M} = [x_{0M}\; y_{0M}\; z_{0M}\; 1]^T \quad (35)$$

An example of the m-file for determining the position vector r_{0M} of the manipulator with the kinematic diagram in Fig. 13 is in Fig. 14.

```
syms q1 q2 q3 q4 L1 L2 L3 L4
T01z3=[1 0 0 0;0 1 0 0;0 0 1 L1;0 0 0 1]
T01z6=[cos(q1) -sin(q1) 0 0;sin(q1) cos(q1) 0 0;0 0 1 0;0 0 0 1]
T01z4=[1 0 0 0;0 0 -1 0;0 1 0 0;0 0 0 1]
T01=T01z3*T01z6*T01z4
%
T12z6=[cos(q2) -sin(q2) 0 0;sin(q2) cos(q2) 0 0;0 0 1 0;0 0 0 1]
T12z1=[1 0 0 L2;0 1 0 0;0 0 1 0;0 0 0 1]
T12=T12z6*T12z1
%
T02=T01*T12
%
T23z6=[cos(q3) -sin(q3) 0 0;sin(q3) cos(q3) 0 0;0 0 1 0;0 0 0 1]
T23z1=[1 0 0 L3;0 1 0 0;0 0 1 0;0 0 0 1]
T23=T23z6*T23z1
%
T03=T01*T12*T23
%
T34z6=[cos(q4) -sin(q4) 0 0;sin(q4) cos(q4) 0 0;0 0 1 0;0 0 0 1]
T34z1=[1 0 0 L4;0 1 0 0;0 0 1 0;0 0 0 1]
T34=T34z6*T34z1
%
T04=T01*T12*T23*T34
%
r4M=[0;0;0;1]
r0M='position vector of point M'
r0M=T04*r4M
x0M_y0M_z0M='component of position vector of point M'
x0M=r0M(1,1)
y0M=r0M(2,1)
z0M=r0M(3,1)
r_0M='magnitude of position vector of point M'
r_0M=sqrt(x0M^2+y0M^2+z0M^2)
```

Figure 14. M-file of the position vector $\mathbf{r_{0M}}$ of point M with D-H parameters

The components of the vector $\mathbf{r_{0M}}$ to individual axes x, y, z determined using Denavit - Hartenberg parameters are shown in Fig. 15. The resulting transformation matrix $\mathbf{T_{04}}$ determined using D-H parameters is shown in Fig. 16.

```
x0M =

L2*cos(q1)*cos(q2) + L4*cos(q4)*(cos(q1)*cos(q2)*cos(q3) - cos(q1)*sin(q2)*sin(q3)) -
L4*sin(q4)*(cos(q1)*cos(q2)*sin(q3) + cos(q1)*cos(q3)*sin(q2)) + L3*cos(q1)*cos(q2)*cos(q3) -
L3*cos(q1)*sin(q2)*sin(q3)

y0M =

L2*cos(q2)*sin(q1) - L4*cos(q4)*(sin(q1)*sin(q2)*sin(q3) - cos(q2)*cos(q3)*sin(q1)) -
L4*sin(q4)*(cos(q2)*sin(q1)*sin(q3) + cos(q3)*sin(q1)*sin(q2)) + L3*cos(q2)*cos(q3)*sin(q1) -
L3*sin(q1)*sin(q2)*sin(q3)

z0M =

L1 + L2*sin(q2) + L4*cos(q4)*(cos(q2)*sin(q3) + cos(q3)*sin(q2)) + L4*sin(q4)*(cos(q2)*cos(q3) -
sin(q2)*sin(q3)) + L3*cos(q2)*sin(q3) + L3*cos(q3)*sin(q2)
```

Figure 15. Components of the position vector r_{0M} to individual axes determined using D-H parameters

The magnitude of the position vector of the point M $|r_{0M}|$ determined using D-H parameters is marked in Fig. 14 as r_0M and is shown in Fig. 17.

```
T04 =

[  cos(q4)*(cos(q1)*cos(q2)*cos(q3) - cos(q1)*sin(q2)*sin(q3)) - sin(q4)*(cos(q1)*cos(q2)*sin(q3) +
cos(q1)*cos(q3)*sin(q2)), - cos(q4)*(cos(q1)*cos(q2)*sin(q3) + cos(q1)*cos(q3)*sin(q2)) -
sin(q4)*(cos(q1)*cos(q2)*cos(q3) - cos(q1)*sin(q2)*sin(q3)),  sin(q1), L2*cos(q1)*cos(q2) +
L4*cos(q4)*(cos(q1)*cos(q2)*cos(q3) - cos(q1)*sin(q2)*sin(q3)) -
L4*sin(q4)*(cos(q1)*cos(q2)*sin(q3) + cos(q1)*cos(q3)*sin(q2)) + L3*cos(q1)*cos(q2)*cos(q3) -
L3*cos(q1)*sin(q2)*sin(q3)]

[ - cos(q4)*(sin(q1)*sin(q2)*sin(q3) - cos(q2)*cos(q3)*sin(q1)) - sin(q4)*(cos(q2)*sin(q1)*sin(q3) +
cos(q3)*sin(q1)*sin(q2)),   sin(q4)*(sin(q1)*sin(q2)*sin(q3) - cos(q2)*cos(q3)*sin(q1)) -
cos(q4)*(cos(q2)*sin(q1)*sin(q3) + cos(q3)*sin(q1)*sin(q2)), -cos(q1), L2*cos(q2)*sin(q1) -
L4*cos(q4)*(sin(q1)*sin(q2)*sin(q3) - cos(q2)*cos(q3)*sin(q1)) - L4*sin(q4)*(cos(q2)*sin(q1)*sin(q3)
+ cos(q3)*sin(q1)*sin(q2)) + L3*cos(q2)*cos(q3)*sin(q1) - L3*sin(q1)*sin(q2)*sin(q3)]

[ cos(q4)*(cos(q2)*sin(q3) + cos(q3)*sin(q2)) + sin(q4)*(cos(q2)*cos(q3) - sin(q2)*sin(q3)),
cos(q4)*(cos(q2)*cos(q3) - sin(q2)*sin(q3)) - sin(q4)*(cos(q2)*sin(q3) + cos(q3)*sin(q2)),      0,
L1 + L2*sin(q2) + L4*cos(q4)*(cos(q2)*sin(q3) + cos(q3)*sin(q2)) + L4*sin(q4)*(cos(q2)*cos(q3) -
sin(q2)*sin(q3)) + L3*cos(q2)*sin(q3) + L3*cos(q3)*sin(q2)]

[       0,       0,       0,       1]
```

Figure 16. The resulting transformation matrix $\mathbf{T_{04}}$

```
r_0M =

((L2*cos(q1)*cos(q2) + L4*cos(q4)*(cos(q1)*cos(q2)*cos(q3) - cos(q1)*sin(q2)*sin(q3)) -
L4*sin(q4)*(cos(q1)*cos(q2)*sin(q3) + cos(q1)*cos(q3)*sin(q2)) + L3*cos(q1)*cos(q2)*cos(q3) -
L3*cos(q1)*sin(q2)*sin(q3))^2 + (L4*cos(q4)*(sin(q1)*sin(q2)*sin(q3) - cos(q2)*cos(q3)*sin(q1)) -
L2*cos(q2)*sin(q1) + L4*sin(q4)*(cos(q2)*sin(q1)*sin(q3) + cos(q3)*sin(q1)*sin(q2)) -
L3*cos(q2)*cos(q3)*sin(q1) + L3*sin(q1)*sin(q2)*sin(q3))^2 + (L1 + L2*sin(q2) +
L4*cos(q4)*(cos(q2)*sin(q3) + cos(q3)*sin(q2)) + L4*sin(q4)*(cos(q2)*cos(q3) - sin(q2)*sin(q3)) +
L3*cos(q2)*sin(q3) + L3*cos(q3)*sin(q2))^2)^(1/2)
```

Figure 17. The magnitude of the position vector $|\mathbf{r_{0M}}|$ of point M

Courses of individual quantities in graphic form are for values L_1 = 0.2[m], L_2 = 0.4[m], L_3 = 0.3[m], L_4 = 0.2[m], ω_{01} = 7 [rad/s], ω_{12} = 0.05 [rad/s], ω_{23} = 0.05 [rad/s], ω_{34} = 0.05 [rad/s], t = (0: 0.05: 15) are shown in Fig. 18 and Fig. 19.

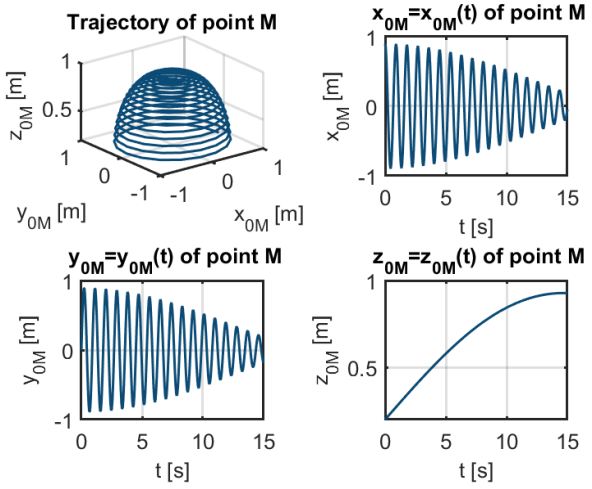

Figure 18. Trajectory components of point M of mechanical system $x_{0M}=f(t)$, $y_{0M}=f(t)$, z_{0M}=f(t)

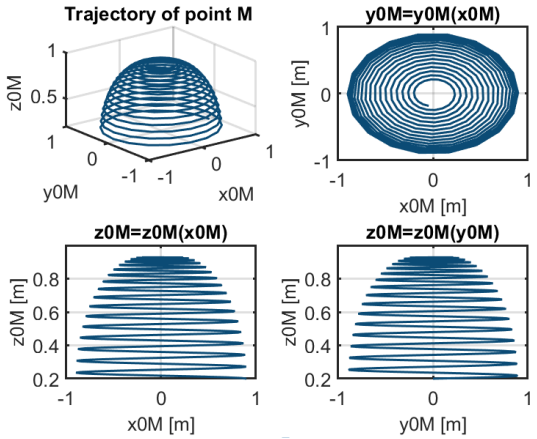

Figure 19. Trajectory components of point M of mechanical y_{0M}=f(x_{0M}), z_{0M}=f(x_{0M}), z_{0M}=f(y_{0M})

The position of the end point M of the manipulator with the kinematic diagram in Fig. 20 is expressed in the following section using the transformation matrices of the basic movements.

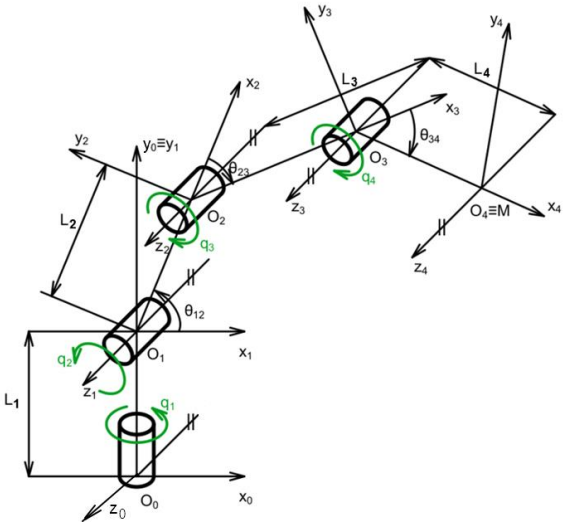

Figure 20. Kinematic scheme of the manipulator RRRR for solving using transformation matrices of basic movements

The transformation between the coordinate system of base 0 and member 1 of the manipulator model in Fig. 20 is described by the matrix $\boldsymbol{T_{01}}$, when $q_1 = \Theta_{01}$, s = sin, c = cos:

$$\boldsymbol{T}_{01} = \boldsymbol{T}_{Z5}\,(q_1)\boldsymbol{T}_{Z2}\,(L_1) \tag{36}$$

$$\boldsymbol{T}_{Z5}\,(q_1) = \begin{bmatrix} c\,q_1 & 0 & s\,q_1 & 0 \\ 0 & 0 & 0 & 0 \\ -s\,q_1 & 0 & c\,q_1 & 0 \\ 0 & 0 & 0 & 1 \end{bmatrix} \tag{37}$$

$$\boldsymbol{T}_{Z2}(L_2) = \begin{bmatrix} 1 & 0 & 0 & 0 \\ 0 & 1 & 0 & L_1 \\ 0 & 0 & 1 & 0 \\ 0 & 0 & 0 & 1 \end{bmatrix} \tag{38}$$

The transformation between the coordinate system of member 1 and member 2 is described by the matrix $\boldsymbol{T_{12}}$, when $q_2 = \Theta_{12}$:

$$\boldsymbol{T}_{12} = \boldsymbol{T}_{Z6}\,(q_2)\boldsymbol{T}_{Z1}\,(L_2) \tag{39}$$

The form of the matrices results from the type of joint:

$$T_{Z6}(q_2) = \begin{bmatrix} c\,q_2 & -s\,q_2 & 0 & 0 \\ s\,q_2 & c\,q_2 & 0 & 0 \\ 0 & 0 & 1 & 0 \\ 0 & 0 & 0 & 1 \end{bmatrix} \quad (40)$$

$$T_{Z1}(L_2) = \begin{bmatrix} 1 & 0 & 0 & L_2 \\ 0 & 1 & 0 & 0 \\ 0 & 0 & 1 & 0 \\ 0 & 0 & 0 & 1 \end{bmatrix} \quad (41)$$

The transformation between the coordinate system of member 2 and member 3 is described by the matrix T_{23}, when $q_3 = \Theta_{23}$:

$$T_{23} = T_{Z6}(q_3)T_{Z1}(L_3) \quad (42)$$

The form of the matrix:

$$T_{Z6}(q_3) = \begin{bmatrix} c\,q_3 & -s\,q_3 & 0 & 0 \\ s\,q_3 & c\,q_3 & 0 & 0 \\ 0 & 0 & 1 & 0 \\ 0 & 0 & 0 & 1 \end{bmatrix} \quad (43)$$

$$T_{Z1}(L_3) = \begin{bmatrix} 1 & 0 & 0 & L_3 \\ 0 & 1 & 0 & 0 \\ 0 & 0 & 1 & 0 \\ 0 & 0 & 0 & 1 \end{bmatrix} \quad (44)$$

The transformation between the coordinate system of member 3 and member 4 is described by a matrix T_{34} when $q_4 = \Theta_{34}$:

$$T_{34} = T_{Z6}(q_4)T_{Z1}(L_4) \quad (45)$$

The form of the matrix:

$$T_{Z6}(q_4) = \begin{bmatrix} c\,q_4 & -s\,q_4 & 0 & 0 \\ s\,q_4 & c\,q_4 & 0 & 0 \\ 0 & 0 & 1 & 0 \\ 0 & 0 & 0 & 1 \end{bmatrix} \quad (46)$$

$$T_{Z1}(L_4) = \begin{bmatrix} 1 & 0 & 0 & L_4 \\ 0 & 1 & 0 & 0 \\ 0 & 0 & 1 & 0 \\ 0 & 0 & 0 & 1 \end{bmatrix} \quad (47)$$

A sample of the m-file for determining the position vector r_{0M} (35) using the transformation matrices of basic movements according to Fig. 21.

```
syms q1 q2 q3 q4 L1 L2 L3 L4
T01z2=[1 0 0 0;0 1 0 L1;0 0 1 0;0 0 0 1]
T01z5=[cos(q1) 0 sin(q1) 0;0 1 0 0;-sin(q1) 0 cos(q1) 0;0 0 0 1]
T01=T01z2*T01z5
%
T12z6=[cos(q2) -sin(q2) 0 0;sin(q2) cos(q2) 0 0;0 0 1 0;0 0 0 1]
T12z1=[1 0 0 L2;0 1 0 0;0 0 1 0;0 0 0 1]
T12=T12z6*T12z1
%
T02=T01*T12
%
T23z6=[cos(q3) -sin(q3) 0 0;sin(q3) cos(q3) 0 0;0 0 1 0;0 0 0 1]
T23z1=[1 0 0 L3;0 1 0 0;0 0 1 0;0 0 0 1]
T23=T23z6*T23z1
%
T03=T01*T12*T23
%
T34z6=[cos(q4) -sin(q4) 0 0;sin(q4) cos(q4) 0 0;0 0 1 0;0 0 0 1]
T34z1=[1 0 0 L4;0 1 0 0;0 0 1 0;0 0 0 1]
T34=T34z6*T34z1
%
T04=T01*T12*T23*T34
%
r4M=[0;0;0;1]
r0M='position vector of point M'
r0M=T04*r4M
x0M_y0M_z0M='component of position vector of point M'
x0M=r0M(1,1)
y0M=r0M(2,1)
z0M=r0M(3,1)
r_0M='magnitude of position vector of point M'
r_0M=sqrt(x0M^2+y0M^2+z0M^2)
```

Figure 21. M-file of the position vector $\mathbf{r_{0M}}$ of point M with trasformation matrix

Position vector $\mathbf{r_{4M}}$ of point M of member 4 in the coordinate system of member 4:

$$T_{12} = T_{Z6}(q_2)T_{Z1}(L_2) \quad (48)$$

The matrix equation of the trajectory of point M with respect to the coordinate system of the base 0:

$$r_{0M} = T_{04}\ r_{4M} \quad (49)$$

The components of the vector $\mathbf{r_{0M}}$ to individual axes x, y, z are shown in Fig. 22.

```
x0M =

L2*cos(q1)*cos(q2) + L4*cos(q4)*(cos(q1)*cos(q2)*cos(q3) - cos(q1)*sin(q2)*sin(q3)) -
L4*sin(q4)*(cos(q1)*cos(q2)*sin(q3) + cos(q1)*cos(q3)*sin(q2)) + L3*cos(q1)*cos(q2)*cos(q3) -
L3*cos(q1)*sin(q2)*sin(q3)

y0M =

L1 + L2*sin(q2) + L4*cos(q4)*(cos(q2)*sin(q3) + cos(q3)*sin(q2)) + L4*sin(q4)*(cos(q2)*cos(q3) -
sin(q2)*sin(q3)) + L3*cos(q2)*sin(q3) + L3*cos(q3)*sin(q2)

z0M =

L4*cos(q4)*(sin(q1)*sin(q2)*sin(q3) - cos(q2)*cos(q3)*sin(q1)) - L2*cos(q2)*sin(q1) +
L4*sin(q4)*(cos(q2)*sin(q1)*sin(q3) + cos(q3)*sin(q1)*sin(q2)) - L3*cos(q2)*cos(q3)*sin(q1) +
L3*sin(q1)*sin(q2)*sin(q3)
```

Figure 22. Components of the position vector $\mathbf{r_{0M}}$ to individual axes

The resulting transformation matrix $\mathbf{T_{04}}$ is shown in Fig. 23.

```
T04 =

[ cos(q4)*(cos(q1)*cos(q2)*cos(q3) - cos(q1)*sin(q2)*sin(q3)) - sin(q4)*(cos(q1)*cos(q2)*sin(q3) +
cos(q1)*cos(q3)*sin(q2)), - cos(q4)*(cos(q1)*cos(q2)*sin(q3) + cos(q1)*cos(q3)*sin(q2)) -
sin(q4)*(cos(q1)*cos(q2)*cos(q3) - cos(q1)*sin(q2)*sin(q3)), sin(q1), L2*cos(q1)*cos(q2) +
L4*cos(q4)*(cos(q1)*cos(q2)*cos(q3) - cos(q1)*sin(q2)*sin(q3)) -
L4*sin(q4)*(cos(q1)*cos(q2)*sin(q3) + cos(q1)*cos(q3)*sin(q2)) + L3*cos(q1)*cos(q2)*cos(q3) -
L3*cos(q1)*sin(q2)*sin(q3)]

[ cos(q4)*(cos(q2)*sin(q3) + cos(q3)*sin(q2)) + sin(q4)*(cos(q2)*cos(q3) - sin(q2)*sin(q3)),
cos(q4)*(cos(q2)*cos(q3) - sin(q2)*sin(q3)) - sin(q4)*(cos(q2)*sin(q3) + cos(q3)*sin(q2)),     0,
L1 + L2*sin(q2) + L4*cos(q4)*(cos(q2)*sin(q3) + cos(q3)*sin(q2)) + L4*sin(q4)*(cos(q2)*cos(q3) -
sin(q2)*sin(q3)) + L3*cos(q2)*sin(q3) + L3*cos(q3)*sin(q2)]

[ cos(q4)*(sin(q1)*sin(q2)*sin(q3) - cos(q2)*cos(q3)*sin(q1)) + sin(q4)*(cos(q2)*sin(q1)*sin(q3) +
cos(q3)*sin(q1)*sin(q2)),   cos(q4)*(cos(q2)*sin(q1)*sin(q3) + cos(q3)*sin(q1)*sin(q2)) -
sin(q4)*(sin(q1)*sin(q2)*sin(q3) - cos(q2)*cos(q3)*sin(q1)), cos(q1),
L4*cos(q4)*(sin(q1)*sin(q2)*sin(q3) - cos(q2)*cos(q3)*sin(q1)) - L2*cos(q2)*sin(q1) +
L4*sin(q4)*(cos(q2)*sin(q1)*sin(q3) + cos(q3)*sin(q1)*sin(q2)) - L3*cos(q2)*cos(q3)*sin(q1) +
L3*sin(q1)*sin(q2)*sin(q3)]

[     0,     0,     0,     1]
```

Figure 23. The resulting transformation matrix $\mathbf{T_{04}}$

The magnitude of the position vector of the point M $|\mathbf{r_{0M}}|$ determined using the methodology is identical to r_0M and is shown in Fig. 17.

The quantities determined by the matrix method are shown graphically in the Matlab program in the next part of the article. For the courses of individual quantities in graphic form, they are for values L_1 = 0.2[m], L_2 = 0.4[m], L_3 = 0.3[m], L_4 = 0.2[m], ω_{01} = 7 [rad/s], ω_{12} = 0.05 [rad/s], ω_{23} = 0.05 [rad/s], ω_{34} = 0.05 [rad/s], t = (0: 0.05: 15) shown in Fig. 24 and Fig. 25.

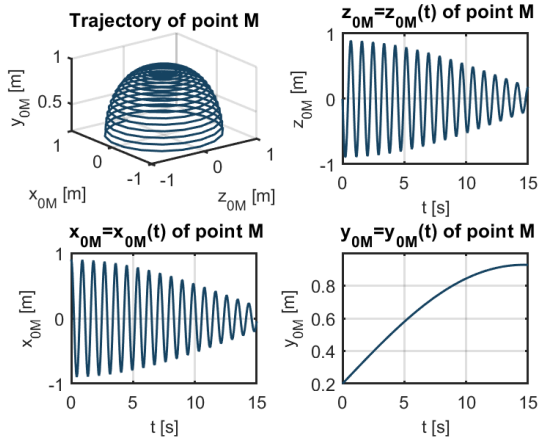

Figure 24. Trajectory components of point M of mechanical system z_{0M}=f(t), x_{0M}=f(t), y_{0M}=f(t)

From $\mathbf{r_{0M}}$ we calculate the velocity $\mathbf{v_{0M}}$ and acceleration $\mathbf{a_{0M}}$ of point M by deriving it according to time in symbolic form with respect to the coordinate system of the base O_0, x_0, y_0, z_0.

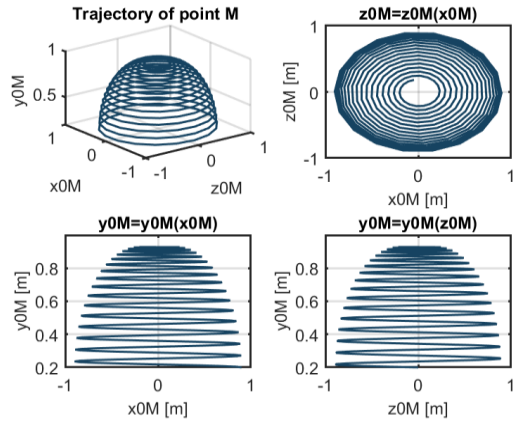

Figure 25. Trajectory components of point M of mechanical z_{0M}=f(x_{0M}), y_{0M}=f(x_{0M}), y_{0M}=f(z_{0M})

8 SOFTWARE SIMULATION

An example of a simulation of a manipulator model with a two-link robotic arm in MSC Adams/View software is presented in this section. The computer model is shown in Fig. 26. The manipulator consists of a stand, two arms of weight m_1 and m_2, length L_1 and L_2, and a working tool. The movable arms are placed on a fixed base. The solid base ensures its stability in operation [Bozek 2021].

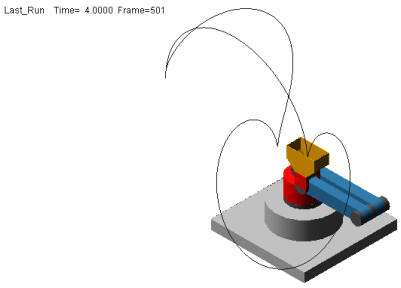

Figure 26. A model of a two-link robotic arm on a fixed base in MSC Adams/View

A working tool, in our case a basket, is attached to the movable arm of the upper part. With the tool, the manipulator performs the required movement. Our goal is to describe the movement of the end member (end-effector). The previous parts of the paper were also devoted to solving the direct task of kinematics (Fig. 27). Postprocessor is a presentation tool for modelling. It is a tool for creating, processing, modifying and presenting simulation results. In the Postprocessor, we can display the model in its current state, and we can also display the simulation results using a file in *.avi format. It also enables the output of numerical values in the form of tables, and we can process numerical results in the form of tables and graphs.
The movement of the arms takes place in the vertical plane, therefore the influence of gravity is also considered. The model does not take into account clearances and frictional effects in the joints. The flexibility of individual arms is not considered either. Driving moments are derived by servo drives in individual kinematic pairs. They ensure the movement of the shoulders. The course of kinematic quantities in graphic form is shown in Fig. 28 and Fig. 29.

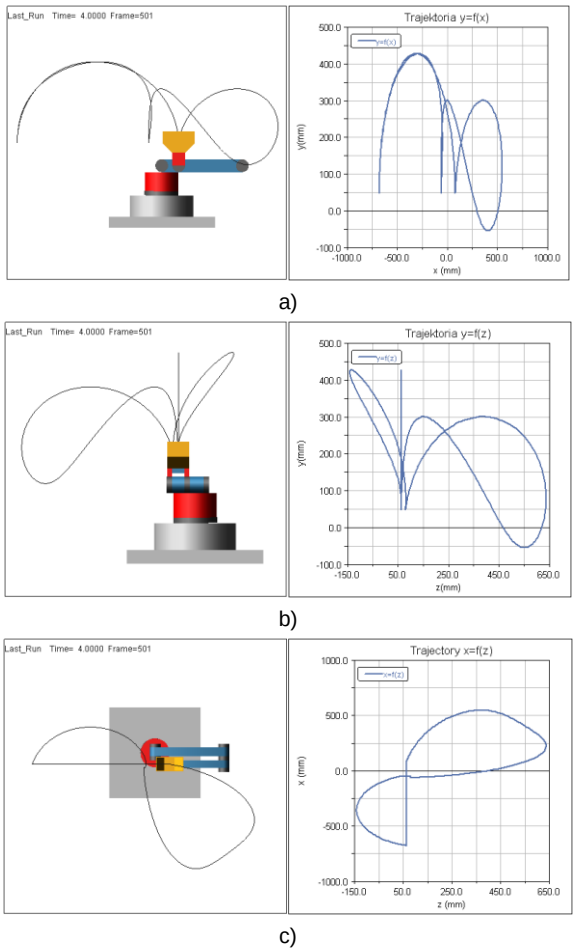

Figure 27. Trajectory of the center of gravity of the end member a) y=f(x), b) y=f(z), c) x=f(z)

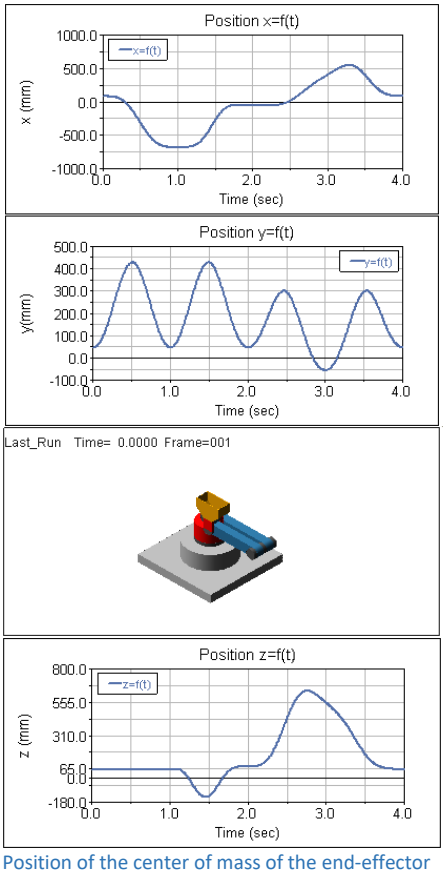

Figure 28. Position of the center of mass of the end-effector a) x_M = f(t), b) y_M = f(t), c) z_M = f(t)

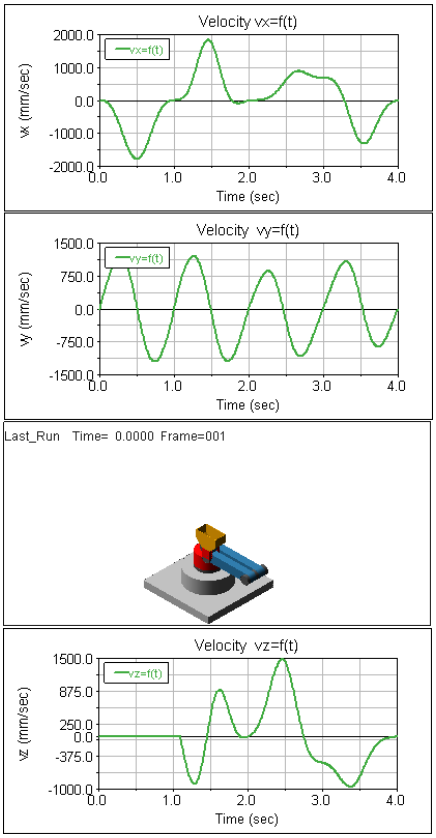

Figure 29. Velocity of the center of mass of the end-effector a) v_{xM} = f(t), b) v_{yM} = f(t), c) v_{zM} = f(t)

9 CONCLUSIONS

The work presented the procedure for solving the kinematic problem of the mechanism in the Matlab program using the matrix method. The direct and inverse problem was solved using matrix methods and the Matlab program. There is also a demonstration of modelling in the MSC Adams View program, which allows simulating the movement of complex mechanical systems such as manipulators.

The advantage of computer simulation is the ability to immediately visualize different solution variants and analyse the effect of possible changes on the function of the model. It allows us to better understand the function of the model and to verify the functionality of the model. Computer simulation enables visualization of the course of movement in real time, which enables verification and notification of possible collisions of elements and displays information on the required indicators on the screen. Interactive simulation and visualization enable convenient modelling work in a mutual connection. Graphs of quantities located in independent windows change with the time of the simulation and thus make it easier to modify the model and subsequently visualize the new resulting quantities.

The tasks are solved numerically. The results are obtained in the form of a time diagram of the required variables. The adoption of this methodology provides us with a suitable tool for solving the problems of teaching and practice. The use of computer software brings economic benefits in addition to time savings. Conditions are being created for faster research and the creation of new mechanical systems gradually appearing in the production area [Kelemen 2014 and 2021, Pirnik 2016, Qazizada 2016, Pavlasek 2018, Zidek 2018, Pivarciova 2019 and 2022, Kurylo 2019, Nikitin 2020, Peterka 2020, Virgala 2020 and 2022, Dyadyura 2021, Kelemenova 2021, Suder 2021].

ACKNOWLEDGMENTS

The authors would like to thank the Slovak Grant Agency - projects VEGA 1/0201/21 and VEGA 1/0436/22.

REFERENCES

[Abramov 2015] Abramov, I. V., Božek, P., Nikitin, J. R., Abramov, A. A., Sosnovich, E. V., Stollmann, V. Diagnostics of electrical drives. In The 18th International Conference on Electrical Drives and Power Electronics. EDPE 2015. Pp. 364-367. DOI: 10.1109/EDPE.2015.7325321.

[Bozek 2014] Bozek, P., Turygin, Y. Measurement of the operating parameters and numerical analysis of the mechanical subsystem. Measurement Science Review, 2014, Vol. 14, No. 4, pp. 198-203.

[Bozek 2021] Bozek, P., Nikitin, Y., Krenicky, T. The Basics Characteristics of Elements Reliability. In: Diagnostics of Mechatronic Systems. Series: Studies in Systems, Decision and Control, 2021, Vol. 345, pp. 1-15. ISBN 978-3-030-67055-9.

[Brat 1981] Brat, V. Matrix methods in the analysis and synthesis of spatially bound mechanical systems. Academia, Prague, 1981.

[Delyova 2014] Delyova, I., et al. Kinematic analysis of crank rocker mechanism using MSC Adams/View. Applied Mechanics and Materials, 2014, Vol. 611, pp. 90-97.

[Dyadyura 2021] Dyadyura, K., Hrebenyk, L., Krenicky, T., Zaborowski, T. Modeling of the Manufacturing Systems State in the Conditions of the Lean Production. MM Science Journal, 2021, Vol. June, pp. 4408-4413.

[Garcia 2015] Garcia, F.J.A., et al. Simulators based on physical modeling tools to support the teaching of automatic control (2): rotary pendulum (Simuladores basados en herramientas de modelado fisico para el apoyo a la enseñanza de control automatico (2): péndulo rotatorio). Actas de las 36 Jornadas de Automatica, 2015, pp. 667-673. (in Spanish)

[Hroncova 2012] Hroncova, D., Binda, M., sarga, P., Kicak, F. Kinematical analysis of crank slider mechanism using MSC Adams/View. Procedia Engineering, 2012, 48, pp. 213-222.

[Hroncova 2014] Hroncova, D., Frankovsky, P., Virgala, I., Delyova, I. Kinematic Analysis of the Press Mechanism Using MSC Adams. American Journal of Mechanical Engineering, 2014, Vol. 2, No. 7, pp. 312-315.

[Karban 2006] Karban, P. Calculations and simulations in Matlab and Simulink programs. Computer Press, Brno, 2006.

[Kelemen 2014] Kelemen, M., et al. Rapid Control Prototyping of Embedded Systems Based on Microcontroller. Procedia Engineering, 2014, Vol. 96, Issue 11, pp. 215-220. ISSN 1877-7058.

[Kelemen 2021] Kelemen, M. et al. Head on Hall Effect Sensor Arrangement for Displacement Measurement. MM Science Journal, 2021, Vol. October, pp. 4757-4763.

[Kelemenova 2021] Kelemenova, T., et al. Verification of Force Transducer for Direct and Indirect Measurements. MM Science Journal, 2021, Vol. October, pp. 4736-4742.

[Kuric 2021] Kuric, I., et al. Analysis of Diagnostic Methods and Energy of Production Systems Drives. Processes, 2021, Vol. 9, Issue 5, DOI:10.3390/pr9050843.

[Kurylo 2019] Kurylo, P., et al. Machine Vision System Measuring the Trajectory of Upper Limb Motion Applying the Matlab Software. Measurement Science Review, 2019, Vol. 19, No. 1, pp. 1-8.

[Mikova 2014] Mikova, L., et al. Simulation Model of Manipulator for Model Based Design. Applied Mechanics and Materials, 2014, Vol. 611, No. 1, pp. 175-182.

[Nikitin 2020] Nikitin, Y., Bozek, P., Peterka, J. Logical-Linguistic Model of Diagnostics of Electric Drives with Sensors Support. Sensors, 2020, Vol. 20, No. 16.

[Nikitin 2022] Nikitin, Y. R., Krenický, T., Božek, P. Diagnostics of automated technological drives. Lüdenscheid: RAM-Verlag, 2022. 148 pp. Monitoring and Analysis of Manufacturing Processes in Automotive Production; Vol. 6. <https://ram-verlag.org/vol-6-diagnostics-of-automated-technological-drives>.

[Pavlasek 2018] Pavlasek, P., et al. Flexible Education Environment: Learning Style Insights to Increase Engineering Students Key Competences. In: Proc. of 10th Int. Conf. on Education and New Learning Technologies EDULEARN18; 2-4 July, 2018; Palma, Spain; 2018, pp. 10156-10165. ISBN 978-84-09-02709-5, 10.21125/edulearn.2018.2468.

[Peterka 2020] Peterka, J., Nikitin, Y., Bozek, P. Diagnostics of automated technological devices. MM Science Journal, 2020, Vol. October, pp. 4027-4034.

[Pirnik 2016] Pirnik, R., Hrubos, M., Nemec, D., Bozek, P. Navigation of the autonomous ground vehicle utilizing low-cost inertial navigation. Acta Mechatronica, 2016, Vol. 1, No. 1, pp. 19-23.

[Pivarciova 2019] Pivarciova, E., Domnina, K., Sagova, Z. Design of the construction and research of vibrations and heat transfer of mine workings. Acta Montanistica Slovaca, 2019, Vol. 24, Issue 1, pp. 15-24.

[Pivarciova 2022] Pivarciova, E. et al. Use of Holographic Interferometry for Monitoring Heat Transfer. MM Science Journal, 2022, Vol. March, pp. 5522-5525.

[Qazizada 2016] Qazizada, M.E., Pivarciova, E. Mobile robot controlling possibilities of inertial navigation system. In: Int. Conf. on Manuf. Engineering and Materials, ICMEM 2016; Novy Smokovec, Slovakia; June 06-10, 2016. Vol. 149, pp. 404-413.

[Saga 2020] Saga, M., et al. Case study: Performance analysis and development of robotized screwing application with integrated vision sensing system for automotive industry. International Journal of Advanced Robotic Systems, 2020, Vol. 17, No. 3.

[Sapietova 2018] Sapietova, A., et al. Application of optimization algorithms for robot systems designing. International Journal of Advanced Robotic Systems, 2018, Vol. 15, No. 1, pp. 1-10.

[Segota 2020] Segota, S., et al. Path planning optimization of six-degree-of-freedom robotic manipulators using evolutionary algorithms. International Journal of Advanced Robotic Systems, 2020, Vol. 17. Issue 2.

[Serrano 2015] Serrano, J., et al. Simulators Based on Physical Modeling Tools to Support the Teaching of Automatic Control (I): Mobile Robot With Flexible Arm (Simuladores Basados en Herramientas de Modelado Fisico Para el Apoyo a la Enseñanza de Control Automatico (I): Robot Móvil Con Brazo Flexible). In: XXXVI Jornadas de Automatica: Libro de Actas, Bilbao, 2015, pp. 659-666. (in Spanish)

[Semjon 2016] Semjon, J., et al. Testing of parameters of proposed robotic wrist based on the precision modules. International Journal of Advanced Robotic Systems, 2016, Vol. 13, pp. 1-7, ISSN 1729-8814.

[Semjon 2020] Semjon, J., et al. Verification of the UR5 robot's properties after a crash caused by a fall of a transferred load from a crane. International Journal of Advanced Robotic Systems, 2016, Vol. 17, Issue 1, pp. 1-9, ISSN 1729-8814.

[Smrcek 2003] Smrcek, J., Palko, A., Nemec, M. Some problems in design of wheeled mobile robot undercarriadge. Acta Mechanica Slovaca, 2003, Vol. 7, Issue 3, pp. 129-136.

[Stejskal 1996] Stejskal, V., Valasek, M. Kinematics and dynamics of Machinery. Marcel Dekker, New York, 1996.

[Suder 2021] Suder, J., et al. Analysis of Increasing the Friction Force of The Robot Jaws by Adding 3D Printed Flexible Inserts. MM Science Journal, 2021, Vol. December, pp. 5322-5326.

[Trojanova 2021] Trojanova, M., Cakurda, T., Hosovsky, A., Krenicky, T. Estimation of Grey-Box Dynamic Model of 2-DOF Pneumatic Actuator Robotic Arm Using Gravity Tests. Applied Sciences, 2021, Vol. 11, No. 10, Art. No. 4490.

[Vagas 2011] Vagas, M., et al. The view to the current state of robotics. International Proceedings of Computer Science and Information Technology, 2011, Vol. 8, pp. 205-209.

[Virgala 2012] Virgala, I., et al. Manipulator End-Effector Position Control. Procedia Engineering, 2012, Vol. 48, pp. 684-692, ISSN 1877-7058.

[Virgala 2014] Virgala, I., et al. Analyzing, Modeling and Simulation of Humanoid Robot Hand Motion. Procedia Engineering, 2014, Vol. 611, pp. 75-82.

[Virgala 2020] Virgala, I. et al. Reconfigurable Wheel-Legged Robot. MM Science Journal, 2020, Vol. June, pp. 3960-3965.

[Virgala 2022] Virgala, I., et al. A Non-Anthropomorphic Bipedal Walking Robot with a Vertically Stabilized Base. Appl. Sci., 2022, Vol. 12, 4108.

[Xiong 2018] Xiong, W., et al. Solution to the motion of a delta manipulator with three degrees of freedom. Ferroelectrics, 2018, Vol. 529, No. 1, pp. 159-167.

[Zidek 2018] Zidek, K., et al. Auxiliary Device for Accurate Measurement by the Smart vision System. MM Science Journal, 2018, Vol. March, pp. 2136-2139.

CONTACTS:

Darina Hroncova, Ing. PhD.
Technical University of Kosice, Faculty of Mechanical Engineering
Institute of Automation, Mechatronics, Robotics and Production Techniques
Letna 9, 04200 Kosice, Slovak Republic
darina.hroncova@tuke.sk